



HAL
open science

Biological Characteristics and Patterns of Codon Usage Evolution for the African Genotype Zika Virus

Martin Faye, Naimah Zein, Cheikh Loucoubar, Manfred Weidmann, Ousmane Faye, Marielton dos Passos Cunha, Paolo de Andrade Zanotto, Amadou Alpha Sall, Oumar Faye

► **To cite this version:**

Martin Faye, Naimah Zein, Cheikh Loucoubar, Manfred Weidmann, Ousmane Faye, et al.. Biological Characteristics and Patterns of Codon Usage Evolution for the African Genotype Zika Virus. *Viruses*, 2020, 12 (11), pp.1306. 10.3390/v12111306 . hal-03698409

HAL Id: hal-03698409

<https://hal.science/hal-03698409>

Submitted on 1 Dec 2022

HAL is a multi-disciplinary open access archive for the deposit and dissemination of scientific research documents, whether they are published or not. The documents may come from teaching and research institutions in France or abroad, or from public or private research centers.

L'archive ouverte pluridisciplinaire **HAL**, est destinée au dépôt et à la diffusion de documents scientifiques de niveau recherche, publiés ou non, émanant des établissements d'enseignement et de recherche français ou étrangers, des laboratoires publics ou privés.

Article

Biological Characteristics and Patterns of Codon Usage Evolution for the African Genotype Zika Virus

Martin Faye ^{1,†}, Naimah Zein ^{2,†}, Cheikh Loucoubar ³, Manfred Weidmann ⁴, Ousmane Faye ¹, Marielton dos Passos Cunha ⁵, Paolo Marinho de Andrade Zanotto ⁵, Amadou Alpha Sall ¹ and Oumar Faye ^{1,*}

¹ Virology Department Institut Pasteur of Dakar, Dakar 220, Senegal; martin.faye@pasteur.sn (M.F.); ousmane.faye@pasteur.sn (O.F.); Amadou.SALL@pasteur.sn (A.A.S.)

² Institute of Genetics and Molecular and Cellular Biology, CEDEX, 10142/67404 Illkirch, France; Naimah.zein@hotmail.fr

³ Bioinformatics, Biostatistics and Modeling group, Institut Pasteur of Dakar, Dakar 220, Senegal; Cheikh.loucoubar@pasteur.sn

⁴ Institute of Aquaculture University of Stirling, Stirling FK9 4LA, Scotland, UK; m.w.weidmann@stir.ac.uk

⁵ Microbiology Department, Institute of Biomedical Sciences, University of São Paulo (USP), São Paulo, SP 05508020, Brazil; marieltondospassos@gmail.com (M.d.P.C.); pzanotto@usp.br (P.M.d.A.Z.)

* Correspondence: Oumar.Faye@pasteur.sn; Tel.: +221-33-839-92-23

† These authors contributed equally to this work.

Received: 8 September 2020; Accepted: 12 October 2020; Published: 14 November 2020



Abstract: We investigated temporal trends of codon usage changes for different host species to determine their importance in Zika virus (ZIKV) evolution. Viral spillover resulting from the potential of codon adaptation to host genome was also assessed for the African genotype ZIKV in comparison to the Asian genotype. To improve our understanding on its zoonotic maintenance, we evaluated in vitro the biological properties of the African genotype ZIKV in vertebrate and mosquito cell lines. Analyses were performed in comparison to Yellow fever virus (YFV). Despite significantly lower codon adaptation index trends than YFV, ZIKV showed evident codon adaptation to vertebrate hosts, particularly for the green African monkey *Chlorocebus aethiops*. PCA and CAI analyses at the individual ZIKV gene level for both human and *Aedes aegypti* indicated a clear distinction between the two genotypes. African ZIKV isolates showed higher virulence in mosquito cells than in vertebrate cells. Their higher replication in mosquito cells than African YFV confirmed the role of mosquitoes in the natural maintenance of the African genotype ZIKV. An analysis of individual strain growth characteristics indicated that the widely used reference strain MR766 replicates poorly in comparison to African ZIKV isolates. The recombinant African Zika virus strain ArD128000*^{E/NS5} may be a good model to include in studies on the mechanism of host tropism, as it cannot replicate in the tested vertebrate cell line.

Keywords: African genotype Zika virus; codon adaptation dynamics; biological characteristics

1. Introduction

Zika virus (ZIKV) is a mosquito-borne *Flavivirus* belonging to the *Flaviviridae* family and the Spondweni serocomplex. ZIKV was first isolated in 1947 in Uganda from a febrile sentinel rhesus monkey during a Yellow fever virus (YFV) study [1]. Its natural transmission cycle involves mainly mosquitoes of the *Aedes* genus and monkeys [2–6], while human infections are accidental and generally asymptomatic. However, in clinical pictures of human infection, the Zika fever (ZF) ranges from a febrile syndrome associated with fever, headache, arthralgia, myalgia, conjunctivitis and cutaneous rash to severe neurological symptoms such as Guillain-Barré syndrome and microcephaly in newborns [7–10].

Overall, sexual intercourse, perinatal infection and blood transfusion have been reported as potential routes of direct transmission of ZIKV among humans [11–13].

The ZIKV genome consists of a linear, single-stranded, positive sense RNA of 10.794 kilobases (Kb) in length. Like other members of the *flavivirus* genus, the polyprotein of ZIKV is flanked by noncoding regions (5' and 3'NCR) and encodes for three structural proteins (5'-C-prM-E-3') and seven nonstructural proteins (5'-NS1-NS2A-NS2B-NS3-NS4A-NS4B-NS5-3'). The envelope (E) and the RNA polymerase (NS5) are major viral proteins mediating binding and membrane fusion and viral replication, respectively [14–16]. ZIKV is associated with a large genetic diversity clustered in three lineages (East African, West African and Asian), and the ZIKV genome has been shown to be subject to recombination and N-glycosylation in nature [17].

Despite serological evidence and entomological data demonstrating ZIKV circulation from 1950s to 1990s, ZIKV remained limited to a sylvatic cycle in equatorial regions of East and West Africa and South-East Asia, with few sporadic human cases [1,18–26]. A ZIKV outbreak in humans occurred in the Yap States of the Federal States of Micronesia in 2007 [27,28]. Subsequently, ZIKV infections were reported in Cambodia and French Polynesia in 2010 and 2013, respectively, and spread to seventy four countries worldwide [29,30]. Since 2013, ZIKV has shown a high prevalence in the Americas and was responsible of a large epidemic in 2015 with Brazil as the epicenter [30–33].

Since the replication cycle of viruses is solely dependent on host translational machinery, efficient viral replication in a host species of usually different genetic background requires a certain degree of genetic adaptation. Thus, mutational and selection pressures can result in adaptation to hosts [34,35]. The Codon Adaptation Index (CAI) is a measure of the synonymous codon usage bias, allowing comparisons of codon usage preferences in different organisms and assessing how well the codon preferences of a virus matches that of a reservoir host or vector [36–38].

Despite several entomological isolations and sporadic human cases reported in different countries in Africa [18,22,39–41], ZF outbreaks in humans have been mostly attributed to the Asian genotype [27–33]. This observation raises the question of whether the adaptation to humans of the African genotype differs from that of Asian genotype. The low public health impact reported for the African genotype ZIKV could be associated with its intrinsic properties. Investigation of the biological and genetic characteristics of African ZIKV strains could improve our understanding of their zoonotic maintenance. Here, we describe an analysis of the codon usage of the African genotype in comparison to the Asian genotype. We also analyze in vitro the biological properties of six ZIKV strains circulating in Africa in mosquito and vertebrate cells. Since ZIKV was first isolated during a Yellow fever disease investigation [1,21,40], and these two viruses share the main vector (*Aedes aegypti*) [2], all analyses and experiments were performed in comparison to YFV, which has a long history of infection in humans and is still a major public health problem, especially in West Africa, where it circulates almost every year [42].

2. Materials and Methods

2.1. Sequence Datasets Analyzed

Nucleotide coding sequences from isolates of ZIKV [$n = 376$ including sequences from African ($n = 20$) and Asian ($n = 356$) genotypes], YFV ($n = 51$) and tobacco mosaic virus (TMV) ($n = 68$) that had information on year and place of isolation and representing all data available to date on Genbank (www.ncbi.nlm.nih.gov/genbank/) were downloaded and used in this study. The complete coding sequences were aligned and curated using Muscle algorithm (<http://www.drive5.com/muscle/>) within the Unipro UGENE software (<http://ugene.net/download.html>) [43].

2.2. Codon Usage Tables

In order to calculate the CAI for the coding regions of the TMV, YFV and ZIKV viruses, we used codon usage tables provided by the CoCoPUTs platform [44,45] for vertebrate hosts including

Homo sapiens, *Macaca mulatta*, *Erythrocebus patas* and *Chlorocebus aethiops*, and invertebrate vectors including *Aedes aegypti*, *Aedes albopictus* and *Culex pipiens* (Table 1).

Table 1. Codon frequency tables for the different hosts considered in the analysis.

| Host Organism | Host | Source | Date of Acquisition | Number of Coding Sequences (CDS) | Number of Codons | Taken from |
|-----------------------------|--------------|----------|---------------------|----------------------------------|------------------|------------|
| <i>Homo sapiens</i> | Vertebrate | CoCoPUTs | 11 June 2019 | 119846 | 78581299 | RefSeq |
| <i>Macaca mulatta</i> | Vertebrate | CoCoPUTs | 20 July 2020 | 67214 | 46960666 | RefSeq |
| <i>Erythrocebus patas</i> | Vertebrate | CoCoPUTs | 20 July 2020 | 165 | 47999 | GenBank |
| <i>Chlorocebus aethiops</i> | Vertebrate | CoCoPUTs | 20 July 2020 | 621 | 183383 | GenBank |
| <i>Aedes aegypti</i> | Invertebrate | CoCoPUTs | 29 May 2019 | 28043 | 20013993 | RefSeq |
| <i>Aedes albopictus</i> | Invertebrate | CoCoPUTs | 20 July 2020 | 37335 | 22045256 | RefSeq |
| <i>Culex pipiens</i> | Invertebrate | CoCoPUTs | 20 July 2020 | 248 | 52907 | GenBank |

2.3. Codon Usage Biases Analysis of Viral Coding Genes

We applied the calculation of the CAI value using a frequency table for vertebrate and invertebrate genes from the CoCoPUTs platform (Table 1) [44,45]. The CAI values were calculated to measure the synonymous codon usage bias using the CAIcal program [46]. To evaluate the statistical support of the CAI values, we defined a threshold value or expected CAI (e-CAI) [47] by generating random sequences with similar GC content, amino acid composition and sequence length to each query sequence (TMV, YFV and ZIKV). CAI values above the e-CAI were interpreted as statistically significant, meaning that codon similarity arose from codon preferences, rather than from internal biases [47].

2.4. Adaptation Levels to Host Genome

In order to assess the adaptation level of the African ZIKV genotype to invertebrate and vertebrates, codon usage of its sequences ($n = 20$) was then analyzed in comparison to the Asian genotype ZIKV ($n = 356$). Sequences of YFV ($n = 51$) and TMV ($n = 68$) were used as positive and negative controls, for adaptation and no adaptation to the human genome, respectively. We also did CAI analyses for each viral coding region using both *A. aegypti* and *H. sapiens* codon usage tables. Additionally, a principal component analysis to verify clustering patterns according to viral genotypes was performed considering the different genomic regions of the virus.

2.5. In Vitro Replication Kinetics of African Zika Virus Strains

2.5.1. Samples

The samples used in this study were provided by the WHO Collaborating Centre for Arboviruses and Hemorrhagic Fevers Reference and Research located at the Institut Pasteur de Dakar in Senegal, and were obtained during a routine surveillance program for multiple mosquito-borne viruses conducted for over 50 years [48]. Strains with evidence of recombination and/or presenting motifs of N-glycosylation on the E protein were included in this study in order to assess the impact of these mechanisms on ZIKV African genotype growth (Table 2).

Table 2. Zika virus strains used in this study.

| Strains | Species | Place of Isolation | Year of Isolation | African Sub-Clades | Number of Passages | Titers of Initial Stocks (PFU/mL) | N-glycosylation Motif (Ng) | Acc. Numbers |
|------------------------------|----------------------------|--------------------|-------------------|--------------------|--------------------|-----------------------------------|----------------------------|-----------------------|
| ArD128000* ^E /NS5 | <i>Aedes luteocephalus</i> | Senegal | 1997 | Nigerian | 4 | 2.5×10^{12} | N-D-T | KF383117 |
| ArD132912 | <i>Aedes dalzieli</i> | Senegal | 1998 | Nigerian | 3 | 1.75×10^7 | N-D-I | KF383021, KF383096 |
| ArD157995* ^E /NS5 | <i>Aedes dalzieli</i> | Senegal | 2001 | Nigerian | 4 | 1.75×10^5 | N-D-I | KF383118 |
| ArD165522 | <i>Aedes vittatus</i> | Senegal | 2002 | Nigerian | 3 | 3.5×10^7 | N-D-I | KF383029, KF383090 |
| MR766 | <i>Macaca mulatta</i> | Uganda | 1947 | Ugandan | 5 | 1.5×10^9 | — | KX421193 |
| HD78788* ^E | <i>Homo sapiens</i> | Senegal | 1991 | Nigerian | 5 | 1.25×10^8 | N-D-T | KF383039, KF383084 |

*^E: Recombinant strain, breakpoints on Envelope (E); *^E/NS5: Recombinant strain, breakpoints on Envelope (E) and polymerase (NS5) proteins (30); Ng: N-glycosylation site at Asn-154 of the Envelope protein (Asn-X-Thr) (25, 30).; Asn: Asparagine (N), Asp: Aspartate (D), Ile: Isoleucine (I), Thr: Threonine (T), “—”: Complete deletion.

2.5.2. Viral Stocks Preparation

Aedes pseudoscutellaris clone 61 (Ap61) continuous cell lines were inoculated with strains used in this study and incubated at 28 °C without CO₂ until a cytopathic effect (CPE) was observable. Infection status was assessed by indirect immunofluorescence assay (IFA) as previously described [49], and virus titers were determined by plaque assay, as previously described [50], using porcine kidney stable cells (PS cells; American Type Culture Collection, Manassas, VA). The supernatants of infected cells were frozen at −80 °C and used as viral stocks for growth kinetics experiments.

2.5.3. Growth Kinetics

An amount of 2.4×10^5 Ap61 or African green monkey kidney epithelial cells (Vero cells; *Cercopithecus aethiops*; Sigma Aldrich, France) were seeded into each well in a volume of 400 µL of appropriate medium [51]. In addition, viral stocks were standardized to the number of plaques forming units per milliliter (PFU/mL), as in previous studies [42,51,52], and cells in each well were infected with 2.4×10^3 plaque-forming units (PFU) of virus in 400 µL of medium, resulting in a multiplicity of infection (MOI) of 0.01. Experiments were conducted in 12-well plates using one plate per virus strain with one uninfected well as a negative control. Plates with infected Ap61 and Vero cells were incubated at 28 °C without CO₂, and at 37 °C with CO₂, respectively. After an incubation time of 4 h, the medium was collected and replaced with 2 mL of new medium to set a start point for the growth kinetics (T0).

At different time points corresponding to 22, 28, 50, 75, 99, 124, and 146 h post infection (hpi), one well per plate was harvested and the supernatants were collected and frozen at −80 °C in small aliquots until use. Cells were washed once with phosphate-buffered saline (PBS) and then collected in 500 µL PBS. A volume of 20 µL of cell suspension was dried on a glass slide for a subsequent immunofluorescence assay [50] to measure viral antigens production; the remaining cell suspensions were frozen at −80 °C. Then, RNA was extracted from cell fractions, and supernatants and copy numbers of the genome were quantified using a real-time reverse transcriptase quantitative polymerase chain reaction (RT-qPCR) and a standard equation previously described for ZIKV quantification [53]. Finally, infectious viral particles were measured in supernatants by plaque assay [50]. The growth kinetics experiments were performed three times on each cell type.

2.5.4. Comparison with Data from In Vitro Growth of YFV

Data of genome production obtained on Ap61 cells during these experiments with ZIKV were also compared to those we previously obtained for YFV in the same conditions with the same MOI as for ZIKV [42] to better understand the zoonotic maintenance of ZIKV. Information about the YFV strains used in the analyses of growth behavior in mosquito cells was provided by the Institut Pasteur de Dakar, WHO Collaborating Center for arboviruses and viral hemorrhagic viruses (CRORA) in Senegal; this data is gathered in Table 3.

Table 3. Yellow fever strains used in analyses of growth behavior.

| Strains | Species | Isolates | Place of Isolation | Year of Isolation | Lineage | Acc. Numbers |
|---------|------------------------|-------------------|--------------------|-------------------|---------|--------------|
| 333 | <i>Aedes aegypti</i> | ArD 114896 | Senegal | 1995 | 3 | JX898871 |
| 307 | <i>Aedes africanus</i> | DakArAmt7 | Côte d'Ivoire | 1973 | 1 | JX898869 |
| 357 | <i>Aedes furcifer</i> | ArD 156468 | Senegal | 2001 | 4 | JX898876 |
| 345 | <i>Aedes furcifer</i> | ArD 149214 | Senegal | 2000 | 5 | JX898873 |
| 314 | <i>Aedes furcifer</i> | ArD 121040 | Senegal | 1996 | 6 | JX898870 |
| Asibi | <i>Homo sapiens</i> | | Ghana | 1927 | | KF769016 |
| 17D | <i>Homo sapiens</i> | 17D RKI #142/94/1 | | | | JN628279 |

2.6. Data Analysis

Perl and R scripts were used to analyze codon usage data in this study, and are available from the authors upon request. In addition, the percentage of immunofluorescence, the logarithm of RNA copy number and the logarithm of viral titers are supposed to be normally distributed, and a Student's test was used to analyze differences between virus strains.

3. Results

3.1. Temporal Trends in CAI Changes to Host Genes

We explored possible changes in CAI over time for YFV and ZIKV using human, monkey and arthropod vector codon usage tables. Both had large numbers of available, serially stamped, complete polyprotein sequences, allowing us to investigate the temporal trends of ZIKV CAI, and to compare differences in the CAI of YFV strains (Figure 1).

YFV demonstrated codon adaptation for both vectors and mammalian hosts across all sampled strains, and the eight CAI trend lines were highly correlated (Spearman's rank correlation test, p -values $< 2.2 \times 10^{-16}$, rho ranging from 0.988 to 0.999). YFV CAI was significantly higher for mammalian than that for vector codon usage (Wilcoxon rank sum test, p -values $< 2.2 \times 10^{-16}$). In addition, YFV CAI was significantly higher for monkeys than for human codon usage (Wilcoxon rank sum test, p -values < 0.00248), and could be associated with the important role of these monkey species in enzootic transmission of YFV. We also observed significant CAI differences between mosquito vectors with higher CAI for *Aedes aegypti* than for *Aedes albopictus* and *Culex pipiens* codon usage (Wilcoxon rank sum test, p -values < 0.0004), indirectly confirming *Aedes aegypti* as the main vector for YFV. No significant differences of YFV CAI were observed for HKgs and AVgs (Wilcoxon rank sum test, p -value = 0.82), or between monkey species (Wilcoxon rank sum test, p -values ranging from 0.461 to 0.560) (Figure 1A).

Similar to YFV, a positive correlation was observed in ZIKV codon adaptation to all eight trend lines (Spearman's rank correlation test, p -values $< 2.2 \times 10^{-16}$, rho ranging from 0.953 to 0.996). However, ZIKV showed a higher CAI towards HKgs than to AVgs (Wilcoxon rank sum test, p -value $< 2.2 \times 10^{-16}$). This effect could have an important impact on the intrinsic biological characteristics of ZIKV during human infection, such as the level of immune response induction.

Across all eight codon usage tables, ZIKV had the highest CAI to *Chlorocebus aethiops* (green African monkey) codon usage (Wilcoxon rank sum test, p -value $< 2.2 \times 10^{-16}$). CAI values were significantly higher for *Aedes aegypti*, the main vector for ZIKV (Wilcoxon rank sum test, p -values $< 2.2 \times 10^{-16}$), and below 1 for *Aedes albopictus* and *Culex pipiens*, indicating no evidence for codon adaptation for these mosquito species (Figure 1B).

On average, ZIKV strains displayed 0.25–0.40 lower CAI values than the YFV strains for all eight codon usage tables tested. In addition, temporal trends have exhibited a variation in ZIKV population size during the last decade, while YFV showed a large population size before the 2000s (Figure 1A,B).

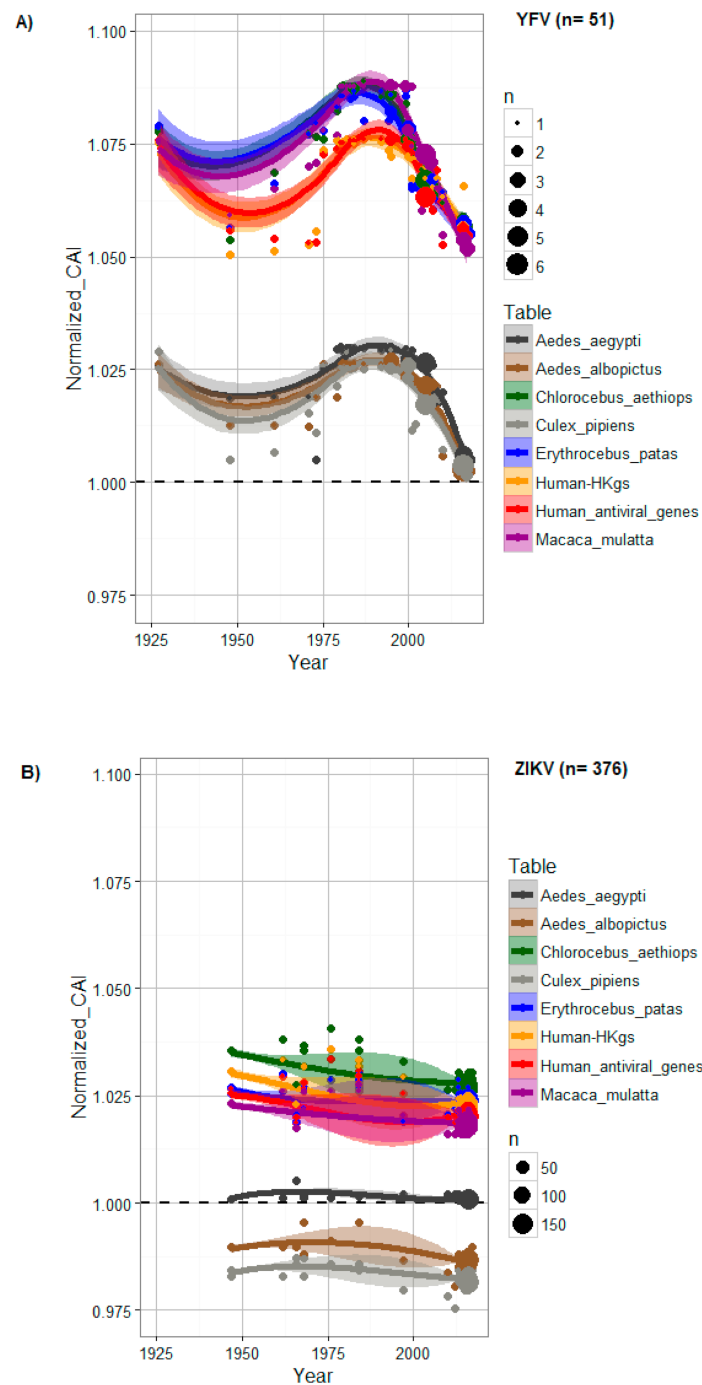


Figure 1. CAI changes to host genes over time for (A) YFV and (B) ZIKV. For each codon usage table, the CAI was normalized by length, percentage of GC and amino acid content for each dataset. The area of the plot points reflects the density of sequences at a specific time point (year). A CAI trend line above 1 (dashed black line) shows evidence of codon adaptation to the host. A trend line was generated using LOESS, a nonparametric regression method, with a 0.95 confidence interval (shaded areas). Data obtained from codon usage tables are colored in dark grey for *Aedes aegypti*, in brown for *Aedes albopictus*, in green for *Chlorocebus aethiops*, in grey for *Culex pipiens*, in blue for *Erythrocebus patas*, in orange for human housekeeping genes (HKGs), in red for highly expressed human antiviral genes (AVGs) and in purple for *Macaca mulatta*.

3.2. CAI Values of Host Genes

The results of the calculation of the CAI values for different hosts, including vertebrates and invertebrates, indicated that ZIKV and YFV had a similar distribution of CAI values for invertebrate vectors and vertebrates, but that ZIKV had slightly lower CAI values than YFV. As expected, both had higher CAI values for all hosts when compared to TMV. Among vertebrate hosts, *Homo sapiens* presented the highest values, considering the distribution of CAI values for both arboviruses tested. For invertebrates, *Aedes aegypti*, followed by *Aedes albopictus*, which are considered to be important vectors for the transmission of arboviruses to vertebrates (Figure 2), had the highest CAI values.

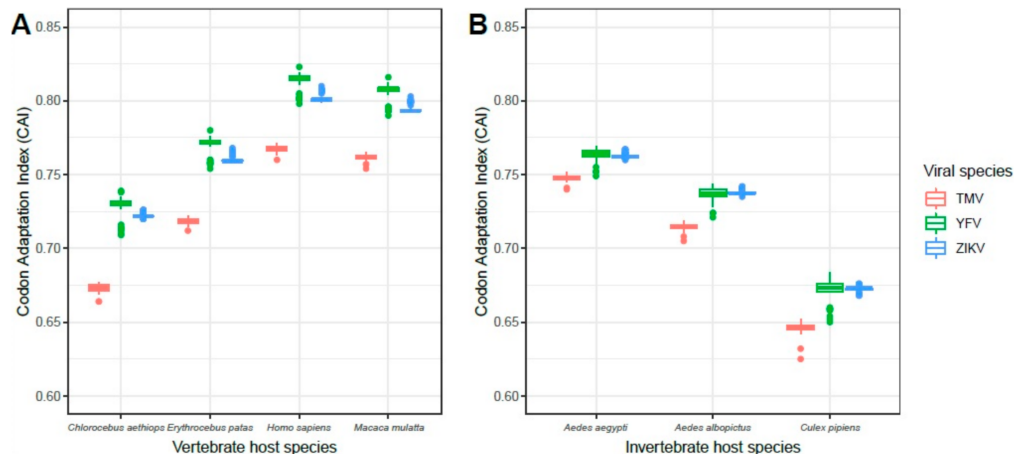


Figure 2. CAI value comparison between ZIKV and YFV to (A) vertebrate hosts and (B) invertebrate vectors. TMV was included as a negative control, since it is not expected to have a codon bias to animals. Data obtained for TMV, YFV and ZIKV are colored in red, green and blue, respectively.

A principal component analysis on hosts with the highest CAI values (*H. sapiens* and *A. aegypti*) indicated a grouping of the two ZIKV genotypes in different groups. This suggested that each genotype may interact with distinct host species (Figure 3). A CAI analysis at the individual ZIKV gene level and/or genomic regions indicated clear differences between the two genotypes. The most evident distinction was observed on the ZIKV coding region for the NS1 protein, which had CAI values higher in the Asian compared to the African genotype for both human and mosquito (Figures 4 and 5).

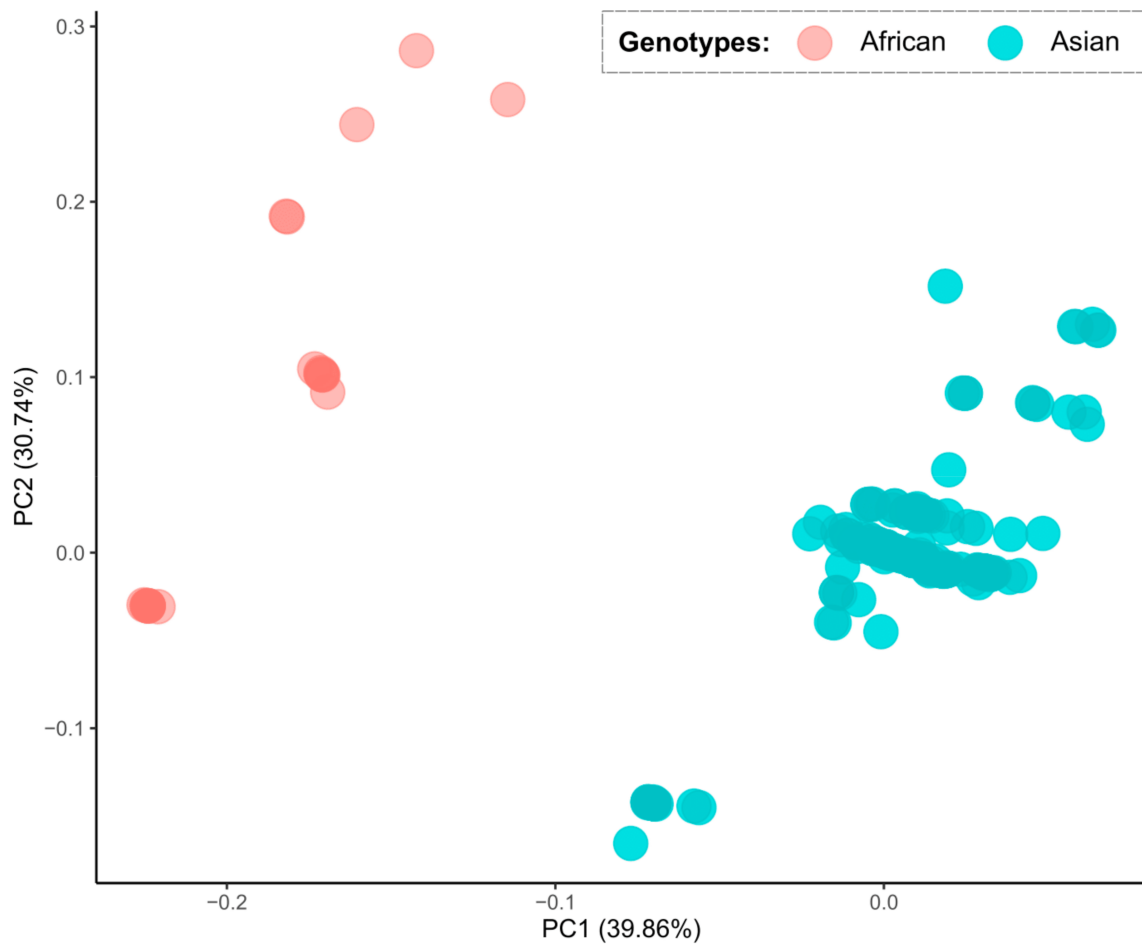


Figure 3. Principal component analysis comparing the CAI values to the *Homo sapiens* and to the *Aedes aegypti* mosquito, comparing between African (red dots) and Asian (blue dots) Zika virus genotypes.

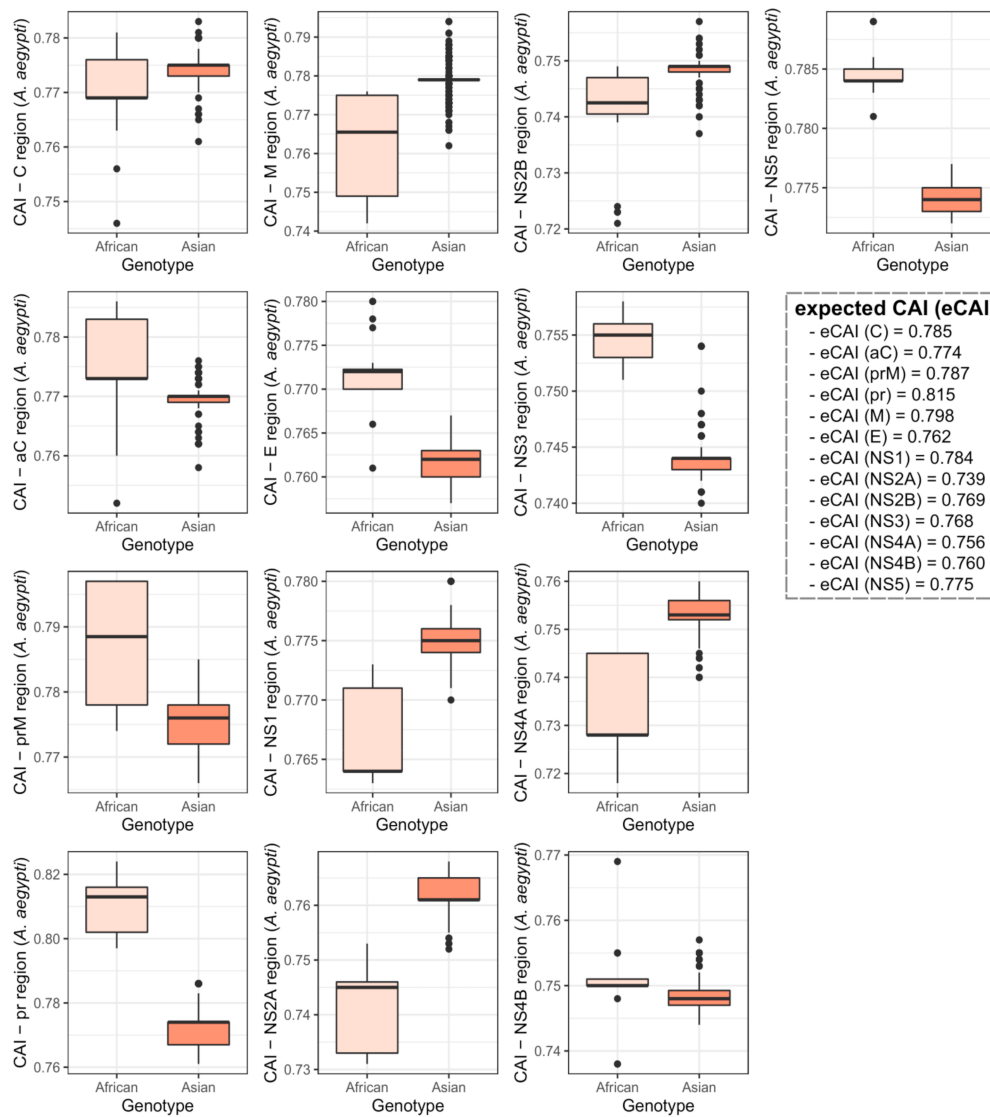


Figure 4. Comparison of the CAI values at the individual ZIKV gene/genomic region levels between the African and Asian ZIKV genotypes to the *Aedes aegypti* mosquito, the main urban ZIKV vector. Data obtained for the African and Asian ZIKV genotypes are colored in light orange and dark orange, respectively.

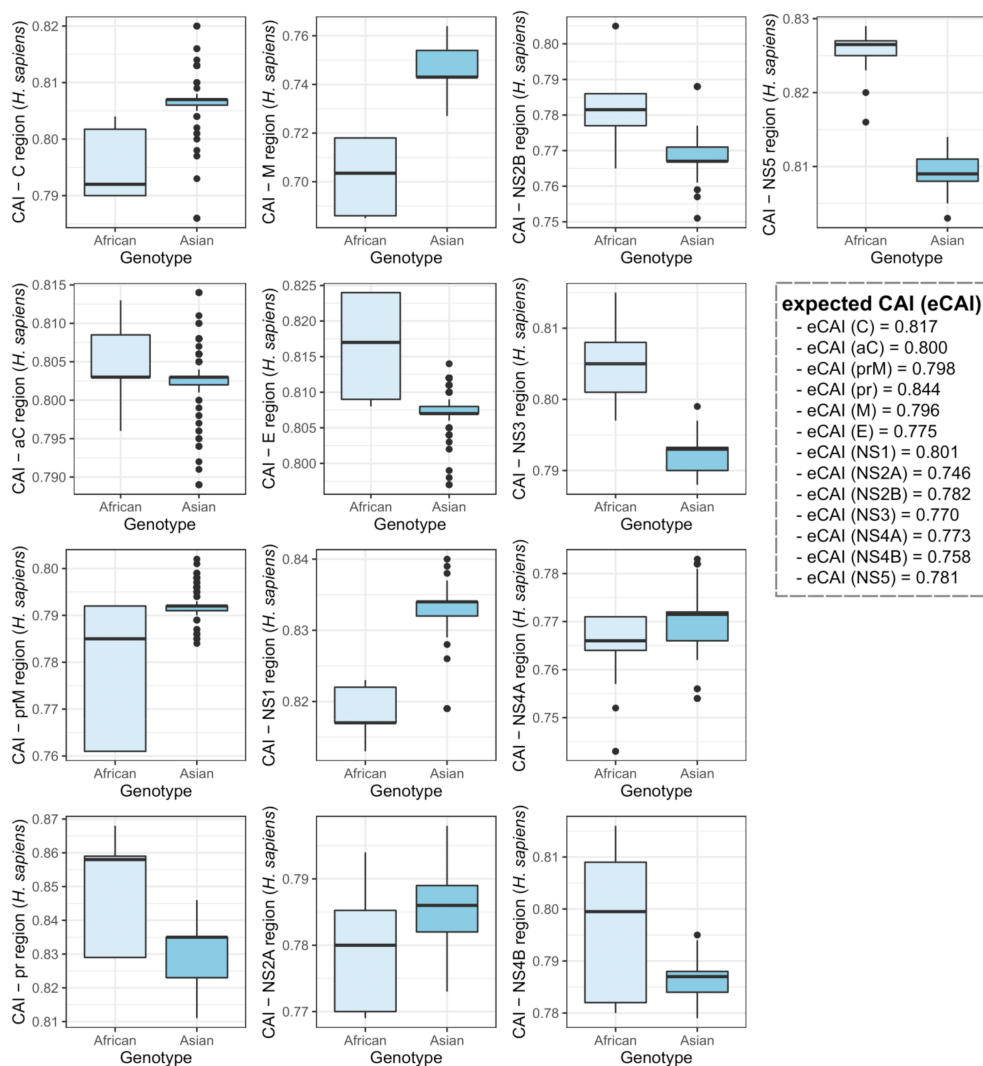


Figure 5. CAI values for the African and Asian ZIKV genotypes to *Homo sapiens* at the individual ZIKV gene/genomic region levels. Data obtained for the African and Asian ZIKV genotypes are colored in light blue and sky blue, respectively.

3.3. In Vitro Growth Kinetics of African ZIKV Strains

In order to understand the biology of the African genotype ZIKV in mosquito vector and vertebrate hosts, the replication kinetics of six African genotype ZIKV strains were determined in AP61 and Vero cells. Infection, viral proliferation and virulence in each cell type were measured by three different tests over a time period of 146 hpi.

We observed that African ZIKV strains had distinct growth dynamics in each cell line. In vertebrate cells, the strains ArD157995^{*E/NS5} and ArD165522 presented a significantly higher production of infectious particles than other African strains from 22 hpi to 50 hpi (p -values ranging from 4.25×10^{-12} to 0.0001). The strain ArD132912 and the human strain HD78788^{*E} showed a production of infectious particles from 75 hpi while the reference monkey strain MR766 released infectious particles very late, i.e., from 99 hpi. Strikingly, we did not detect any infectious particles for the strain ArD128000^{*E/NS5} isolated from a mosquito over a period of 146 hpi (p -values ranging from 9.26×10^{-10} to 4.79×10^{-1}). However, no significant difference was found between other African ZIKV strains from 75 hpi to 146 hpi (Figure 6A). The highest replication after 146 hpi was recorded for strains ArD157995^{*E/NS5}, ArD165522 and ArD132912, which showed similar growth dynamics. Significantly reduced replication efficiency was observed for the reference strain MR766, reduced replication for the human strain HD78788^{*E}

and the mosquito strain ArD128000^{*E/NS5} (Figure 6C,E). The strains ArD157995^{*E/NS5}, ArD165522, ArD132912 and ArD128000^{*E/NS5} showed a higher efficiency in the production of viral antigens, while the reference monkey strain MR766 and the human strain HD78788^{*E} were characterized by significant lower production of viral proteins at 124 hpi and 146 hpi (p -values ranging from 7.32×10^{-15} to 0.0001) (Figure 6G).

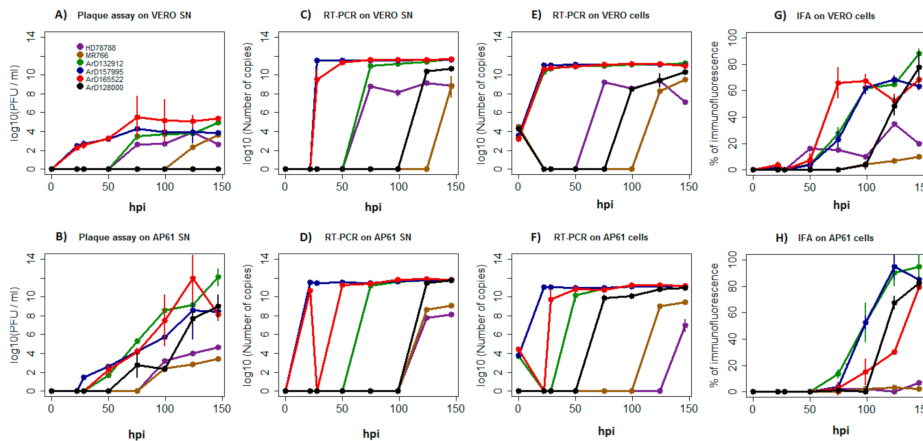


Figure 6. Growth kinetics of African Zika virus strains. The strain label is in reference to the strains in Table 2. Figure 6A–H show the number of infectious viral particles (A and B) (\log_{10} of PFU/mL), the amount of viral RNA equivalents isolated from supernatants (C and D) and cell fractions (E and F) (\log_{10} of RNA copy number), and the percentage (%) of immunofluorescence of viral antigen production (G and H) over a time period of 146 h post infection (hpi). The experiments were performed using the vertebrate cell line Vero (top row) and the mosquito cell line Ap61 (bottom row). Cells were infected with the human strain HD78788^{*E}, the reference monkey strain MR766 and the mosquito strains ArD165522, ArD132912, ArD157995^{*E/NS5}, ArD128000^{*E/NS5} colored in purple, brown, green, blue, red and black, respectively. The error bars indicate the range in values of three independent experiments performed using a multiplicity of infection (MOI) of 0.01.

In mosquito cells, the mosquito strains ArD165522, ArD132912, ArD157995^{*E/NS5} and ArD128000^{*E/NS5} displayed higher infectious particle production, while the reference monkey strain MR766 and the human strain HD78788^{*E} released significantly reduced amounts of infectious particles from 124 hpi to 146 hpi (p -values ranging from 3.75×10^{-8} to 0.011) (Figure 6B). More efficient genome replication was also recorded for the mosquito strains ArD165522, ArD132912, ArD157995^{*E/NS5} and ArD128000^{*E/NS5}, while the vertebrate strains MR766 and strain HD78788^{*E} replicated much less over 146 hpi (p -values ranging from 6.19×10^{-9} to 0.0001) (Figure 6D,F). Similar differences were also observed for viral antigens production, in which the reference monkey strain MR766 and the human strain HD78788^{*E} showed also lower significant rates than the other ZIKV strains from 124 hpi to 146 hpi (p -values ranging from 9.44×10^{-7} to 1.13×10^{-1}) (Figure 6H).

Furthermore, cell line-specific culture differences were observed among African ZIKV strains. Despite quiet similar quantities of viral particles being released into the supernatants by each strain in both cell lines, African ZIKV strains produced up to 4 \log_{10} more infectious viral particles in mosquito cells than in vertebrate cells (Figure 6A,B); this indicates differing replication efficiencies in both cell lines or even incomplete replication (Figure 6A–D). For example, infectious particles for the strain ArD128000^{*E/NS5} were not detected in supernatants from the vertebrate cells over a time period of 146 hpi, while the titer of infectious particles (PFU/mL) increased significantly in mosquito cell supernatants (p -values ranging from 2.63×10^{-12} to 0.035) (Figure 6A,B).

Cell-specific replication differences were obvious for strain ArD165522, which showed a significant decrease at harvesting times 22 hpi and 28 hpi in cell fractions and supernatants from mosquito cells, respectively, while it presented high replication rates in the vertebrate cell line during the corresponding

time points (p -values ranging from 3.75×10^{-10} to 0.027). In addition, the human strain HD78788^{*E} released fewer RNA copies into supernatants from mosquito cells over 146 hpi, while we found a significantly higher genome copy number in supernatants from vertebrate cells (p -values ranging from 9.26×10^{-10} to 4.79×10^{-3}) (Figure 6C–F). Significantly lower profiles of viral antigen production were also observed for the human strain HD78788^{*E} and the monkey strain MR766 in both cell lines when compared to the ZIKV strains ArD165522, ArD132912 and ArD157995^{*E/NS5} (p -values ranging from 7.32×10^{-15} to 0.002) and the strain ArD128000^{*E/NS5}, which showed a significant increase in viral antigen production in both cell lines from 99 hpi to 146 hpi (p -values ranging from 2.51×10^{-11} to 6.08×10^{-4}) (Figure 6G,H).

In summary, the African ZIKV strains exhibited distinct growth characteristics in each cell line, and especially in the mosquito cell line. These differences seem to be associated with their host species origin, as the human strain HD78788^{*E} and the monkey strain MR766 were more cell-specific; both replicated more abundantly in vertebrate cells (Figure 6A–H), while the mosquito strains ArD165522, ArD132912, ArD157995^{*E/NS5} and ArD128000^{*E/NS5} displayed a more efficient growth in mosquito cells regarding the production of infectious particles (Figure 6A,B).

Among recombinant ZIKV strains, we observed different profiles. The E and NS5 recombinant strain ArD157995^{*E/NS5} replicated more efficiently in both vertebrate and mosquito cell lines. The E and NS5 recombinant strain ArD128000^{*E/NS5} exhibited an intermediate replication profile in both cell lines, while the E recombinant strain HD78788^{*E} presented much lower growth dynamics, particularly in mosquito cells (p -values ranging from 1.59×10^{-13} to 0.019) (Figure 6A–H). These different replication profiles may be associated with recombination in the NS5 protein or the simultaneous presence of recombination in both the E and NS5 proteins, since strains presenting these changes replicated more abundantly than the E recombinant strain HD78788^{*E}. However, the replication levels of recombinant strains were not significantly distinct from those of nonrecombinant strains, considering the presence of profiles with more or less efficient replication in both groups.

Interestingly, the strains ArD165522, ArD132912 and ArD157995^{*E/NS5}, presenting the N-glycosylation motif NDI at Asparagine 154 of the E protein, showed more efficient growth replication than strains ArD128000^{*E/NS5} and HD78788^{*E} with NDT motif or the strain MR766, which showed complete deletion of that motif (p -values ranging from 3.11×10^{-10} to 0.001). This effect was more marked in the vertebrate cell line, and showed that N-glycosylation on the E protein can play a major role in changes during growth of African ZIKV strains (Figure 6A–H).

Finally, we estimated the replication efficiency by finding the ratios of the number of plaque forming units divided by the total number of particles released in the supernatants (PFU/mL/Particles) from each time point for each strain in each cell line. We found significant differences in replication efficiency with much higher and increasing ratios over 146 hpi observed in mosquito cells (p -values ranging from 6.32×10^{-16} to 0.0013) (Figure 7A,B). African ZIKV strains produced more infectious viral particles in mosquito cells than in vertebrate cells. This effect was very pronounced for the recombinant strain ArD128000^{*E/NS5}, which produced no infectious particles at all in Vero cells over 146 hpi (Figure 7A,B). Reference monkey strain MR766 was shown to be the least efficient of all the ZIKV strains tested in both cell lines.

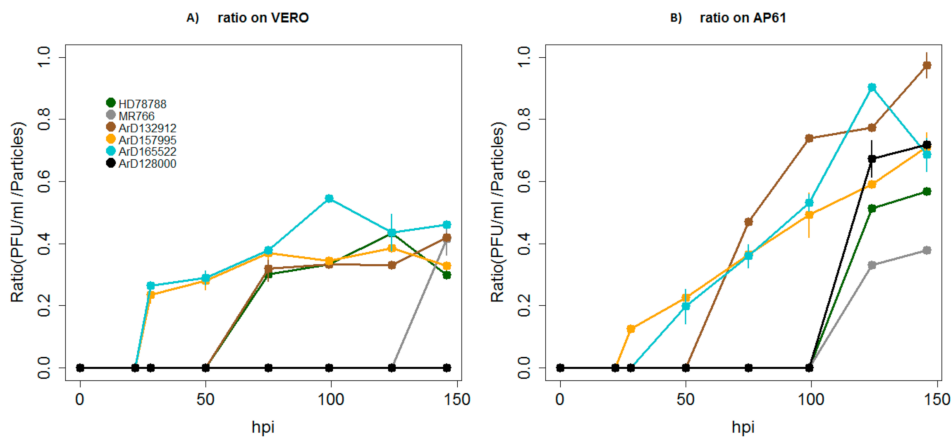


Figure 7. Ratios of the number of plaque forming units of African Zika virus divided by the total number of particles released in the supernatants (PFU/mL/Particles) in vertebrate cells Vero (A) and mosquito cells Ap61 (B) cell lines. The strain label is in reference to the strains in Table 2. Figure 4A,B shows the replication efficiency for each strain in each cell line (A and B) over a time period of 146 h post infection (hpi). Ratios for the human strain HD78788^E are colored in green, the reference monkey strain MR766 is represented in dark gray line and the mosquito strains ArD165522, ArD132912, ArD157995^{E/NS5} and ArD128000^{E/NS5} are highlighted in brown, orange, light blue and black, respectively.

3.4. Replication Growth of African YFV

Since YFV and ZIKV share the same main vector, i.e., *Aedes aegyti*, their growth behaviors were compared in mosquito AP61 cells.

The growth dynamics of African YFV showed that strains 307, 357, 345 and 314 (belonging to lineages 1, 4, 5 and 6, respectively) exhibited high growth efficiency regarding the number of RNA copies and infectious particles produced in mosquito cells. The reference wild-type strain Asibi and the attenuated vaccine strain 17D replicated less efficiently, while strain 333 (lineage 3) displayed the lowest replication efficiency (Figure 8A–C).

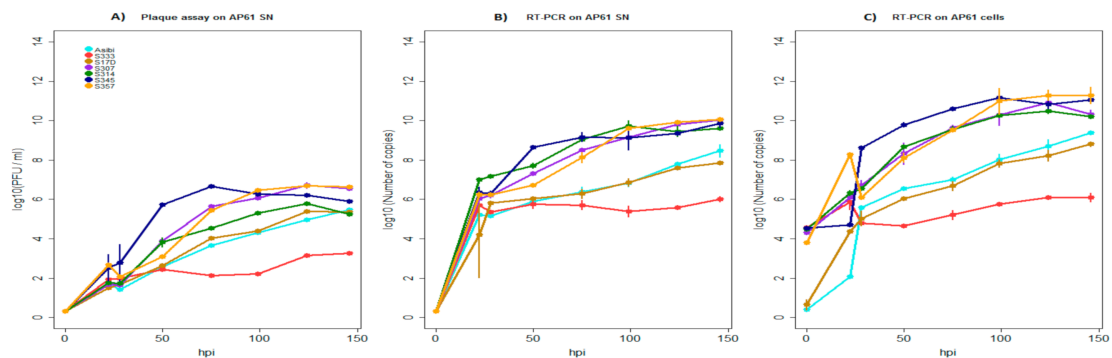


Figure 8. Replication growth kinetics of African Yellow Fever virus on mosquito cells (Ap61). Figure 8A–C show the number of infectious viral particles (A) (log₁₀ of PFU/mL), the amount of viral genome copies quantified from supernatants (B) and cells (C) (Log₁₀ of RNA copy number) over a time period of 146 h post infection (hpi). The strain label is in reference to the strains in Table 3. Data obtained with the reference wild-type strain Asibi are colored in light blue and the curves in red, brown, purple, green, dark blue and orange represent strains 333, 17D, 307, 314, 345 and 357, respectively. The error bars indicate the range in values of three independent experiments performed using a multiplicity of infection (MOI) of 0.01.

In comparison to YFV strains, the growth of African ZIKV strains in mosquito cells was much slower, but with the exception of the human strain HD78788^{*E}, all African ZIKV strains replicated more abundantly (from 2 to 6Log₁₀) than YFV strains and produced significantly more infectious particles in cell supernatants (*p*-values ranging from 5.02×10^{-6} to 0.001) (Figure 6B–F and Figure 8A–C). These results suggest a high-titer virus production for the African genotype ZIKV in *Aedes* mosquito cells, which could play an important role in its natural maintenance.

4. Discussion

As seen for YFV and West Nile virus (WNV), first isolated in Africa, ZIKV is another flavivirus which spread from Africa to other continents [2,17]. The genetic diversity and broad host range of ZIKV [54] might have contributed to its extensive dissemination, and the A188V substitution in the NS1 protein of Asian ZIKV strain may be key to ZIKV spread from southeastern Asia across the Pacific islands to the Americas [55,56]. Its natural transmission cycle mainly involves monkeys, arboreal mosquitoes and, occasionally, humans.

The evolutionary adjustment of viruses to hosts through codon usage adaptation may reveal the role of host in natural maintenance of particular viruses.

Temporal analyses of CAI are informative in better identifying time points, which were marked by advantageous nonsynonymous changes in different hosts. Despite low CAI changes observed in its evolution, ZIKV shows slow evolutionary dynamics just like those of YFV [17,36,57,58]. Nevertheless, this slow evolution dynamic might be helpful for efficient replication of RNA viruses in the host, as more than one codon can be used for the same amino acid [56,59,60]. The significant lower CAI to AVgs than to HKgs could be linked to the ability of ZIKV to evade the immune system, in addition to inhibiting IFN production, as previously reported [61]. In addition, the higher CAI of ZIKV to *Chlorocebus aethiops* (green African monkey) is not surprising, because several monkey species have been identified as primary reservoirs of ZIKV [62], and therefore this monkey species could be involved in sylvatic ZIKV transmission in Africa. However, the recent detection of ZIKV in neotropical primates (*Sapajus libidinosus*) highlights the possibility that other host species could be involved in a sustained sylvatic cycle in the Americas [63], but perhaps also in Africa, and their role in ZIKV maintenance needs to be understood.

The abrupt variation observed in ZIKV population sizes over time could be correlated to the rapid increase of available sequencing data [64] and to the recent wide distribution of ZIKV from the Pacific Islands to the Americas [30–33]. The high NS1 CAI values of the Asian genotype for the human genome confirmed in this study were associated with the Asian genotype ZIKV for humans [65].

The lower CAI values obtained for the *Aedes aegypti* mosquito vector could explain the low competence for ZIKV for *Aedes aegypti* in the Americas [66] or the insignificant ZIKV transmission by *Aedes aegypti* in Africa, where it is transmitted by several other *Aedes spp.* mosquitoes, such as *Aedes vittatus* and *Aedes luteocephalus* [6]; this raises the question of the main *Aedes* vector for ZIKV in Africa.

Despite multiple isolations from mosquito populations and serological evidence of ZIKV infection in Africa, a major outbreak in humans attributed to the African genotype ZIKV has not yet been documented. Codon bias is a common mechanism across the genomes of several organisms and plays a major role in their evolution. The significant ZIKV adaptation to the genome of monkeys could lead to possible spillover of the African genotype ZIKV to other vertebrates such as humans, as exhibited by the high CAI for the human genome, which is actually already higher than the CAI of Asian genotype ZIKV. This clearly shows that the African genotype ZIKV also has the potential to efficiently replicate in humans. This is particularly true for the CAI for the E and NS5 proteins [65], which have a major role in flaviviruses replication and virulence [17].

African genotype ZIKV presents two major clades, which have previously experienced probable recombination and glycosylation mechanisms in their natural cycle [17,28]. To better understand its biology in mosquito vectors and vertebrate hosts and assess the effect of these evolutionary mechanisms on its fitness, the in vitro phenotypical behavior of African ZIKV strains was analyzed over a 146 hpi

period. Thus, infection, viral proliferation and virulence in each cell type were assessed using RT-qPCR of the lysed cell fraction to measure genome replication, RT-qPCR of the supernatant fraction to detect genome replication dynamics (i.e., total number of particle released), plaque assays to determine the amount of infectious viral particles (PFU/mL) from the supernatant fraction, and immunofluorescence staining of the cells to estimate efficiency in viral antigen production.

While some differences were previously reported between African and Asian ZIKV strains [66–70], our study focuses on phenotypic differences between African ZIKV strains by characterizing their growth behaviors in two distinct cell lines. The observed high-titer virus production in mosquito cells and significantly reduced levels in vertebrate cells may reflect ZIKV maintenance in African transmission cycles.

The replication levels of African ZIKV strains isolated from mosquitoes in the vertebrate cell line confirms that these isolates are able to efficiently infect and replicate in vertebrate cells, as, for example, reported for neuronal cells [70,71]. However, the lower replication efficiency in the vertebrate cell line might contribute to the inability of African genotype ZIKV to cause severe pathogenicity in vertebrates such as humans.

Indeed, the African genotype ZIKV has been shown to induce less pathogenicity in human cells than the epidemic Asian genotype ZIKV, which shows long-term persistence, more consistent with clinical manifestations [72–74]. The reduced pathogenicity exhibited by the African genotype ZIKV in human cells in vitro was correlated with the induction of early cell death and a strong antiviral response [41,48,70,71,75], which explains the low amount of infectious viral particles produced in vertebrate cells in our study.

African ZIKV strains are more virulent in mosquito cells [76]. This observation is supported by our assessment of replication efficiency in a mosquito cell line (PFU/mL/Particles), shown in Figure 4.

However, cell-specific phenotypic differences observed between African ZIKV strains used in our study might be related to the intrinsic properties of the African ZIKV strains, their species origin or differential susceptibility to ZIKV infection for the cell lines used in our study [77–79]. Indeed, mosquito strains ArD157995^{*E/NS5}, ArD165522, ArD132912 and ArD128000^{*E/NS5} replicated more efficiently in the mosquito cell line, while the human strain HD78788^{*E} and the monkey strain MR766 showed higher replication in the vertebrate cell line. It is of note that the prototype ancestral ZIKV strain MR766 replicated significantly more slowly. At least three MR766 strains exist with genetic differences [80]. Our results indicate that strain MR766, which is used in the majority of ZIKV research studies, cannot be considered as a reference, as it shows quite atypical ZIKV replication in both vertebrate and mosquito cells.

Like other RNA viruses cycling between arthropod vector and mammal hosts, it was previously found that the majority of codon sites in E and NS5 proteins of ZIKV undergo purifying selection [17,51,81]. Nevertheless, some significant diversifying sites exist in the genome of the African genotype ZIKV, such as recombination sites in E and NS5 proteins and the N-glycosylation motif (NDT) at codon positions 154–156 of the E protein, which plays a crucial role in the replication and virulence of flaviviruses [17,51,52,82,83]. Although recombination could not be associated with one specific replication profile of African ZIKV strains in our study, the significant replication difference between strains ArD128000^{*E/NS5} and HD78788^{*E}, particularly in mosquito cells, points to the detrimental impact of recombination in the NS5 protein on virulence and viral infectivity. The effect of recombination on replication efficiency and virulence of ZIKV has long been suspected based on phylogenetic studies [17,84,85]. The recombinant strain ArD128000^{*E/NS5}, which replicated efficiently in mosquito cells but exhibited no production of infectious particles in the vertebrate cell line over 146 hpi, indicated that recombination has an effect on host tropism.

In contrast to a previous in vivo study demonstrating that complete deletion—as observed in most of the African ZIKV strains—or single amino acid substitution in the NDT motif cause less infectivity [86], our study shows that the NDI motif at codon position 156 of the E protein is an important determinant of the virulence and replication of African ZIKV strains in vertebrate cells.

The recombination and N-glycosylation may lead to potential future adaptation and pathogenicity of the African genotype ZIKV, and the biological and genetic characteristics of new isolates need to be continuously monitored.

However, considering functional differences between in vitro and in vivo systems in terms of physical barriers and antiviral responses, the fitness of African ZIKV strains with a NDI motif on the E protein should be studied in vivo, since many other amino acid substitutions contributing to ZIKV pathogenicity have been previously identified [87–89]. Enhanced infectivity of ZIKV in the *Aedes aegypti* mosquito vector has been correlated with the signature A188V mutation in NS1, which potentially facilitates transmission, and therefore, contributed to the spread of the virus from Asia to the Americas [88,89].

In contrast to faster in vitro replication of African YFV in mosquito cells, the African ZIKV strains exhibited more efficient replication, yielding more infectious particles. In contrast to YFV, which has a long history of human infection in Africa [42,90], the African genotype ZIKV currently appears to be maintained through a sylvatic cycle, and human infections still appear to be rare. However, our own serological data from active surveillance of arboviruses in Senegal indicate that asymptomatic ZIKV infections may be more widespread than assumed [91]. If confirmed, asymptomatic or unnoticed infection could be an alternative explanation for the higher CAI values for the human genome of the African genotype ZIKV.

In summary African genotype ZIKV isolates replicate more efficiently in mosquito cells than in vertebrate cells. Their CAI indices, however, indicate a higher adaptation to vertebrates than observed for Asian genotype ZIKV, which may reflect efficient sylvatic transmission cycles but possibly also asymptomatic transmission in a peri-urban cycle. An analysis of the growth characteristics of individual African genotype ZIKV strains revealed that strain MR766 is not suitable as a reference strain, while recombinant strain ArD128000^{*E/NS5} may be a good model for use studies on the mechanism of host tropism.

Author Contributions: M.F., N.Z., A.A.S., O.F. (Ousmane Faye) and O.F. (Oumar Faye) conceived and designed the experiments; M.F. and N.Z. performed the experiments. M.F., N.Z., C.L. and O.F. (Ousmane Faye) analyzed and interpreted the data. M.F. performed the temporal trends analysis. M.d.P.C. and P.M.d.A.Z. performed CAI and PCA analysis. M.F., N.Z. and M.W. were major contributors in writing the manuscript. All authors have read and agree to the published version of the manuscript.

Funding: This research received no specific grant from any funding agency in the public, commercial, or not-for-profit sectors and was only supported by the Institut Pasteur de Dakar.

Acknowledgments: We acknowledge colleagues of virology pole of Institut Pasteur de Dakar, Senegal for sharing mosquito pools and supportive information necessary for establishment and accomplishment of this study. We also thank Nicholas di Paola (Center for Genome Sciences, United States Army Medical Research Institute of Infectious Diseases (USAMRIID), Fort Detrick, Frederick, Maryland, USA.) for sharing codon usage tables for human genes. This work was also made possible by the tripartite (I. Pasteur, USP, FIOCRUZ) ZIKV project.

Conflicts of Interest: The authors declare no conflict of interest. The supporting sponsors had no role in the design of the study; in the collection, analyses, or interpretation of data; in the writing of the manuscript, and in the decision to publish the results.

References

1. Dick, G.W.; Kitchen, S.F.; Haddow, A.J. Zika virus isolations and serological specificity. *Trans. R. Soc. Trop. Med. Hyg.* **1952**, *46*, 509–520. [[CrossRef](#)]
2. Hayes, E.B. Zika virus outside Africa. *Emerg. Infect. Dis.* **2009**, *15*, 1347–1350. [[CrossRef](#)] [[PubMed](#)]
3. Weinbren, M.P.; Williams, M.C. Zika virus: Further isolations in the Zika area and some studies on the strains isolated. *Trans. R. Soc. Trop. Med. Hyg.* **1958**, *52*, 263–268. [[CrossRef](#)]
4. Haddow, A.J.; Williams, M.C.; Woodall, J.P.; Simpson, D.I.H.; Goma, L.K. Twelve isolations of Zika virus from *Aedes (Stegomyia) africanus* (Theobald) taken in and above a Ugandan forest. *Bull. World Health Organ.* **1964**, *31*, 57–69. [[PubMed](#)]
5. Marchette, N.J.; Garcia, R.; Rudnick, A. Isolation of Zika virus from *Aedes aegypti* mosquitoes in Malaysia. *Am. J. Trop. Med. Hyg.* **1969**, *18*, 411–415. [[CrossRef](#)] [[PubMed](#)]

6. Diagne, C.T.; Diallo, D.; Faye, O.; Ba, Y.; Faye, O.; Gaye, A.; Dia, I.; Faye, O.; Weaver, S.C.; Sall, A.A.; et al. Potential of selected Senegalese *Aedes spp.* mosquitoes (Diptera: *Culicidae*) to transmit Zika virus. *BMC Infect. Dis.* **2015**, *15*, 492. [[CrossRef](#)] [[PubMed](#)]
7. Wertheim, H.F.; Horby, P.; Woodall, J.P. *Atlas of Human Infectious Diseases*; John Wiley & Sons: Hoboken, NJ, USA, 2012.
8. Chan, J.F.; Choi, G.K.; Yip, C.C.; Cheng, V.C.; Yuen, K.Y. Zika fever and congenital Zika syndrome: An unexpected emerging arboviral disease. *J. Infect.* **2016**, *72*, 507–524. [[CrossRef](#)] [[PubMed](#)]
9. Al-Qahtani, A.A.; Nazir, N.; Al-Anazi, M.R.; Rubino, S.; Al-Ahdal, M.N. Zika virus: A new pandemic threat. *J. Infect. Dev. Ctries.* **2016**, *10*, 201–207. [[CrossRef](#)]
10. Ramos da Silva, S.; Gao, S.J. Zika virus: An update on epidemiology, pathology, molecular biology, and animal model. *J. Med. Virol.* **2016**, *88*, 1291–1296. [[CrossRef](#)]
11. Besnard, M.; LastÃre, S.; Teissier, A.; Cao-Lormeau, V.M.; Musso, D. Evidence of perinatal transmission of Zika virus, French Polynesia, December 2013 and February 2014. *Eurosurveillance* **2014**, *19*, 20751. [[CrossRef](#)]
12. Slavov, S.N.; Otaguiri, K.K.; Kashima, S.; Covas, D.T. Overview of Zika virus (ZIKV) infection in regards to the Brazilian epidemic. *Braz. J. Med. Biol. Res.* **2016**, *49*, e5420. [[CrossRef](#)] [[PubMed](#)]
13. Foy, B.D.; Kobylinski, K.C.; Foy, J.L.C.; Blitvich, B.J.; da Rosa, A.T.; Haddock, A.D.; Lanciotti, R.S.; Tesh, R.B. Probable non-vector-borne transmission of Zika virus, Colorado, USA. *Emerg. Infect. Dis.* **2011**, *17*, 880–882. [[CrossRef](#)] [[PubMed](#)]
14. Lindenbach, B.D.; Rice, C.M. Molecular biology of flaviviruses. *Adv. Virus Res.* **2003**, *59*, 23–61. [[PubMed](#)]
15. Chambers, T.J.; Chang, H.S.; Galler, R.; Rice, C.M. Flavivirus genome organization, expression and replication. *Ann. Rev. Micro* **1990**, *44*, 649–688. [[CrossRef](#)] [[PubMed](#)]
16. Kuno, G.; Chang, G.J. Full-length sequencing and genomic characterization of Bagaza, Kedougou, and Zika viruses. *Arch. Virol.* **2007**, *152*, 687–696. [[CrossRef](#)] [[PubMed](#)]
17. Faye, O.; Freire, C.C.; Iamarino, A.; Faye, O.; de Oliveira, J.V.; Diallo, M.; Zanutto, P.M.; Sall, A.A. Molecular evolution of Zika virus during its emergence in the 20(th) century. *PLoS Negl. Trop. Dis.* **2014**, *8*, e2636. [[CrossRef](#)] [[PubMed](#)]
18. Fagbami, A.H. Zika virus infections in Nigeria: Virological and seroepidemiological investigations in Oyo State. *J. Hyg. (Lond.)* **1979**, *83*, 213–219. [[CrossRef](#)]
19. Robin, Y.; Mouchet, J. Serological and entomological study on yellow fever in Sierra Leone. *Bull. Soc. Pathol. Exot. Fil.* **1978**, *68*, 249–258.
20. Jan, C.; Languillat, G.; Renaudet, J.; Robin, Y. A serological survey of arboviruses in Gabon. *Bull. Soc. Pathol. Exot. Fil.* **1978**, *71*, 140–146.
21. McCrae, A.W.; Kirya, B.G. Yellow fever and Zika virus epizootics and enzootics in Uganda. *Trans. R. Soc. Trop. Med. Hyg.* **1982**, *76*, 552–562. [[CrossRef](#)]
22. Saluzzo, J.F.; Gonzalez, J.P.; Herve, J.P.; Georges, A.J. Serological survey for the prevalence of certain arboviruses in the human population of the south-east area of Central African Republic. *Bull. Soc. Pathol. Exot. Fil.* **1981**, *74*, 490–499.
23. Monlun, E.; Zeller, H.; Le Guenno, B.; Traore-Lamizana, M.; Hervy, J.P.; Adam, F.; Ferrara, L.; Fontenille, D.; Sylla, R.; Mondo, M. Surveillance of the circulation of arbovirus of medical interest in the region of eastern Senegal. *Bull. Soc. Pathol. Exot.* **1993**, *86*, 21–28. [[PubMed](#)]
24. Akoua-Koffi, C.; Diarrassouba, S.; Benie, V.B.; Ngbichi, J.M.; Bozoua, T.; Bosson, A.; Akran, V.; Carnevale, P.; Ehouman, A. Investigation surrounding a fatal case of yellow fever in Côte d'Ivoire in 1999. *Bull. Soc. Pathol. Exot.* **2001**, *94*, 227–230. [[PubMed](#)]
25. Darwish, M.A.; Hoogstraal, H.; Roberts, T.J.; Ahmed, I.P.; Omar, F. A seroepidemiological survey for certain arboviruses (*Togaviridae*) in Pakistan. *Trans. R. Soc. Trop. Med. Hyg.* **1983**, *77*, 442–445. [[CrossRef](#)]
26. Olson, J.G.; Ksiazek, T.G.; Suhandiman, T. Zika virus, a cause of fever in Central Java, Indonesia. *Trans. R. Soc. Trop. Med. Hyg.* **1981**, *75*, 389–393. [[CrossRef](#)]
27. Duffy, M.R.; Chen, T.H.; Hancock, W.T.; Powers, A.M.; Kool, J.L.; Lanciotti, R.S.; Pretrick, M.; Marfel, M.; Holzbauer, S.; Dubray, C.; et al. Zika virus outbreak on Yap Island, Federated States of Micronesia. *N. Engl. J. Med.* **2009**, *360*, 2536–2543. [[CrossRef](#)]
28. Lanciotti, R.S.; Kosoy, O.L.; Laven, J.J.; Velez, J.O.; Lambert, A.J.; Johnson, A.J.; Stanfield, S.M.; Duffy, M.R. Genetic and serologic properties of Zika virus associated with an epidemic, Yap State, Micronesia, 2007. *Emerg. Infect. Dis.* **2008**, *14*, 1232–1239. [[CrossRef](#)]

29. Heang, V.; Yasuda, C.Y.; Sovann, L.; Haddow, A.D.; da Rosa, A.P.T.; Tesh, R.B.; Kasper, M.R. Zika virus infection, Cambodia, 2010. *Emerg. Infect. Dis.* **2012**, *18*, 349–351. [[CrossRef](#)]
30. World Health Organization. Epidemiological Update Zika Virus Infection. 2015. Available online: http://www.paho.org/hq/index.php?option=com_docman&task=doc_view&Itemid=270&gid=32021&lang=en (accessed on 14 October 2020).
31. Zanluca, C.; Melo, V.C.; Mosimann, A.L.; Santos, G.I.; Santos, C.N.; Luz, K. First report of autochthonous transmission of Zika virus in Brazil. *Mem. Inst. Oswaldo Cruz.* **2015**, *110*, 569–572. [[CrossRef](#)]
32. Magalhães-Barbosa, M.C.; Prata-Barbosa, A.; Robaina, J.R.; Raymundo, C.E.; Lima-Setta, F.; Cunha, A.J. Trends of the microcephaly and Zika virus outbreak in Brazil, January–July 2016. *Travel. Med. Infect. Dis.* **2016**, *14*, 458–463. [[CrossRef](#)]
33. Demir, T.; Kilic, S. Zika virus: A new arboviral public health problem. *Folia Microbiol. (Praha)* **2016**, *61*, 523–527. [[CrossRef](#)] [[PubMed](#)]
34. Hussain, S.; Rasool, S.T. Analysis of Synonymous Codon Usage in Zika Virus. *Acta Tropica.* **2017**. [[CrossRef](#)] [[PubMed](#)]
35. Singh, N.K.; Tyagi, A. A detailed analysis of codon usage patterns and influencing factors in Zika virus. *Arch. Virol.* **2017**, *162*, 1963–1973. [[CrossRef](#)] [[PubMed](#)]
36. Sharp, P.M.; Li, W.H. The codon Adaptation Index- a measure of directional synonymous codon usage bias, and its potential applications. *Nucleic Acids Res.* **1987**, *15*, 1281–1295. [[CrossRef](#)]
37. Sharp, P.M.; Tuohy, T.M.; Mosurski, K.R. Codon usage in yeast: Cluster analysis clearly differentiates highly and lowly expressed genes. *Nucleic Acids Res.* **1986**, *14*, 5125–5143. [[CrossRef](#)]
38. Carbone, A.; Zinovyev, A.; Képès, F. Codon adaptation index as a measure of dominating codon bias. *Bioinformatics* **2003**, *19*, 2005–2015. [[CrossRef](#)]
39. Diallo, D.; Sall, A.A.; Diagne, C.T.; Faye, O.; Faye, O.; Ba, Y.; Hanley, K.A.; Buenemann, M.; Weaver, S.C.; Diallo, M. Zika virus emergence in mosquitoes in southeastern Senegal, 2011. *PLoS ONE* **2014**, *9*, e109442. [[CrossRef](#)]
40. Macnamara. Zika virus: A report on three cases of human infection during an epidemic of jaundice in Nigeria. *Trans. R. Soc. Trop. Med. Hyg.* **1954**, *48*, 139–145. [[CrossRef](#)]
41. Grard, G.; Caron, M.; Mombo, I.M.; Nkoghe, D.; Mboui, O.S.; Jiolle, D.; Fontenille, D.; Paupy, C.; Leroy, E.M. Zika virus in Gabon (Central Africa)–2007: A new threat from *Aedes albopictus*? *PLoS Negl. Trop. Dis.* **2014**, *8*, e2681. [[CrossRef](#)]
42. Stock, N.K.; Laraway, H.; Faye, O.; Diallo, M.; Niedrig, M.; Sall, A.A. Biological and phylogenetic characteristics of yellow fever virus lineages from West Africa. *J. Virol.* **2013**, *87*, 2895–2907. [[CrossRef](#)]
43. Okonechnikov, K.; Golosova, O.; Fursov, M. The UGENE team. Unipro UGENE: A unified bioinformatics toolkit. *Bioinformatics* **2012**, *28*, 1166–1167. [[CrossRef](#)] [[PubMed](#)]
44. Athey, J.; Alexaki, A.; Osipova, E.; Rostovtsev, A.; Santana-Quintero, L.V.; Katneni, U.; Simonyan, V.; Kimchi-Sarfaty, C. A new and updated resource for codon usage tables. *BMC Bioinform.* **2017**, *18*, 391. [[CrossRef](#)] [[PubMed](#)]
45. Alexaki, A.; Kames, J.; Holcomb, D.D.; Athey, J.; Santana-Quintero, L.V.; Lam, P.V.N.; Hamasaki-Katagiri, N.; Osipova, E.; Simonyan, V.; Bar, H.; et al. Codon and Codon-Pair Usage Tables (CoCoPUTs): Facilitating Genetic Variation Analyses and Recombinant Gene Design. *J. Mol. Biol.* **2019**, *431*, 2434–2441. [[CrossRef](#)] [[PubMed](#)]
46. Puigbo, P.; Bravo, I.G.; Garcia-Vallve, S. CAIcal: A combined set of tools to assess codon usage adaptation. *Biol. Direct.* **2008**, *3*, 38. [[CrossRef](#)] [[PubMed](#)]
47. Puigbo, P.; Bravo, I.G.; Garcia-Vallve, S. E-CAI: A novel server to estimate an expected value of Codon Adaptation Index (eCAI). *BMC Bioinform.* **2008**, *9*, 65. [[CrossRef](#)] [[PubMed](#)]
48. Althouse, B.M.; Hanley, K.A.; Diallo, M.; Sall, A.A.; Ba, Y.; Faye, O.; Diallo, D.; Watts, D.M.; Weaver, S.C.; Cummings, D.A. Impact of climate and mosquito vector abundance on sylvatic arbovirus circulation dynamics in Senegal. *Am. J. Trop. Med. Hyg.* **2015**, *92*, 88–97. [[CrossRef](#)] [[PubMed](#)]
49. Digoutte, J.P.; Calvo-Wilson, M.A.; Mondo, M.; Traore-Lamizana, M.; Adam, F. Continuous cell lines and immune ascitic fluid pools in arbovirus detection. *Res. Virol.* **1992**, *143*, 417–422. [[CrossRef](#)]
50. De Madrid, A.T.; Porterfield, J.S. A simple micro-culture method for the study of group B arboviruses. *Bull. World Health Organ.* **1969**, *40*, 113–121.

51. Fall, G.; Di Paola, N.; Faye, M.; Dia, M.; de Melo Freire, C.C.; Loucoubar, C.; de Andrade Zanotto, P.M.; Faye, O. Biological and phylogenetic characteristics of West African lineages of West Nile virus. *PLoS Negl. Trop. Dis.* **2017**, *11*, e0006078. [[CrossRef](#)]
52. Hanna, S.L.; Pierson, T.C.; Sanchez, M.D.; Ahmed, A.A.; Murtadha, M.M.; Doms, R.W. N-linked glycosylation of west nile virus envelope proteins influences particle assembly and infectivity. *J. Virol.* **2005**, *79*, 13262–13274. [[CrossRef](#)]
53. Faye, O.; Faye, O.; Diallo, D.; Diallo, M.; Weidmann, M.; Sall, A.A. Quantitative real-time PCR detection of Zika virus and evaluation with field-caught mosquitoes. *Virol. J.* **2013**, *10*, 311. [[CrossRef](#)]
54. Bueno, M.G.; Martinez, N.; Abdalla, L.; Nunes, D.d.S.C.; Chame, M. Animals in the Zika Virus Life Cycle: What to Expect from Megadiverse Latin American Countries. *PLoS Negl. Trop. Dis.* **2016**, *10*, e0005073. [[CrossRef](#)]
55. Delatorre, E.; Mir, D.; Bello, G. Tracing the origin of the NS1 A188V substitution responsible for recent enhancement of Zika virus Asian genotype infectivity. *Mem. Inst. Oswaldo Cruz.* **2017**. [[CrossRef](#)]
56. Althouse, B.M.; Vasilakis, N.; Sall, A.A.; Diallo, M.; Weaver, S.; Hanley, K.A. Potential for Zika virus to establish a sylvatic transmission cycle in the Americas. *BioRxiv* **2016**, in press. [[CrossRef](#)]
57. Ciota, A.T.; Bialosuknia, S.M.; Ehrbar, D.J.; Kramer, L.D. Vertical Transmission of Zika Virus by *Aedes aegypti* and *Ae. albopictus* Mosquitoes. *Emerg. Infect. Dis.* **2017**, *23*, 880–882. [[CrossRef](#)] [[PubMed](#)]
58. Sall, A.A.; Faye, O.; Diallo, M.; Firth, C.; Kitchen, A.; Holmes, E.C. Yellow fever virus exhibits slower evolutionary dynamics than dengue virus. *J. Virol.* **2010**, *84*, 765–772. [[CrossRef](#)] [[PubMed](#)]
59. Bryant, J.E.; Holmes, E.C.; Barrett, A.D.T. Out of Africa: A molecular perspective on the introduction of yellow fever virus into the Americas. *PLoS Pathog.* **2007**, *3*, 0668–0673. [[CrossRef](#)] [[PubMed](#)]
60. Chen, Y.; Shi, Y.; Deng, H.; Gu, T.; Xu, J.; Ou, J.; Jiang, Z.; Jiao, Y.; Zou, T.; Wang, C. Characterization of the porcine epidemic diarrhea virus codon usage bias. *Infect. Genet. Evol.* **2014**, *28*, 95–100. [[CrossRef](#)] [[PubMed](#)]
61. Colavita, F.; Bordoni, V.; Caglioti, C.; Biava, M.; Castilletti, C.; Bordi, L.; Quartu, S.; Iannetta, M.; Ippolito, G.; Agrati, C.; et al. ZIKV Infection Induces an Inflammatory Response but Fails to Activate Types I, II, and III IFN Response in Human PBMC. *Mediat. Inflamm.* **2018**, 2450540. [[CrossRef](#)]
62. Vorou, R. Zika virus, vectors, reservoirs, amplifying hosts, and their potential to spread worldwide: What we know and what we should investigate urgently. *Int. J. Inf. Dis.* **2016**, *48*, 85–90. [[CrossRef](#)]
63. Favoretto, S.; Araujo, D.; Oliveira, D.; Duarte, N.; Mesquita, F.; Zanotto, P.; Durigon, E. First detection of Zika virus in neotropical primates in Brazil: A possible new reservoir. *bioRxiv* **2016**, 049395. [[CrossRef](#)]
64. Shi, M.; Lin, X.D.; Vasilakis, N.; Tian, J.H.; Li, C.X.; Chen, L.J.; Eastwood, G.; Diao, X.N.; Chen, M.H.; Chen, X.; et al. Divergent Viruses Discovered in Arthropods and Vertebrates Revise the Evolutionary History of the Flaviviridae and Related Viruses. *J. Virol.* **2015**, *90*, 659–669. [[CrossRef](#)] [[PubMed](#)]
65. Freire, C.; Palmisano, G.; Braconi, C.T.; Cugola, F.R.; Russo, F.B.; Beltrão-Braga, P.C.; Iamarino, A.; Lima Neto, D.F.; Sall, A.A.; Rosa-Fernandes, L.; et al. NS1 codon usage adaptation to humans in pandemic Zika virus. *Mem. Inst. Oswaldo Cruz.* **2018**, *113*, e170385. [[CrossRef](#)] [[PubMed](#)]
66. Chouin-Carneiro, T.; Vega-Rua, A.; Vazeille, M.; Yebakima, A.; Girod, R.; Goindin, D.; Dupont-Rouzeyrol, M.; Lourenço-de-Oliveira, R.; Failloux, A.B. Differential susceptibilities of *Aedes aegypti* and *Aedes albopictus* from the Americas to Zika virus. *PLoS Negl. Trop. Dis.* **2016**, *10*, 1–11. [[CrossRef](#)] [[PubMed](#)]
67. Garcez, P.P.; Loiola, E.C.; Madeiro, d.C.R.; Higa, L.M.; Trindade, P.; Delvecchio, R.; Nascimento, J.M.; Brindeiro, R.; Tanuri, A.; Rehen, S.K. Zika virus impairs growth in human neurospheres and brain organoids. *Science* **2016**, *352*, 816–818. [[CrossRef](#)]
68. Qian, X.; Nguyen, H.N.; Song, M.M.; Hadiono, C.; Ogden, S.C.; Hammack, C.; Yao, B.; Hamersky, G.R.; Jacob, F.; Zhong, C.; et al. Brain-region-specific organoids using mini-bioreactors for modeling ZIKV exposure. *Cell* **2016**, *165*, 1238–1254. [[CrossRef](#)]
69. Lazear, H.M.; Govero, J.; Smith, A.M.; Platt, D.J.; Fernandez, E.; Miner, J.J.; Diamond, M.S. A mouse model of Zika virus pathogenesis. *Cell Host Microbe* **2016**, *19*, 720–730. [[CrossRef](#)]
70. Zhang, F.; Hammack, C.; Ogden, S.C.; Cheng, Y.; Lee, E.M.; Wen, Z.; Qian, X.; Nguyen, H.N.; Li, Y.; Yao, B.; et al. Molecular signatures associated with ZIKV exposure in human cortical neural progenitors. *Nucleic Acids Res.* **2016**, *44*, 8610–8620. [[CrossRef](#)]
71. Anfasa, F.; Siegers, J.Y.; van der Kroeg, M.; Mumtaz, N.; Raj, V.S.; de Vrij, F.M.S.; Widagdo, W.; Gabriel, G.; Salinas, S.; Simonin, Y.; et al. Phenotypic Differences between Asian and African Lineage Zika Viruses in Human Neural Progenitor Cells. *mSphere* **2017**, *2*, e00292-17. [[CrossRef](#)]

72. Simonin, Y.; Loustalot, F.; Desmetz, C.; Foulongne, V.; Constant, O.; Fournier-Wirth, C.; Leon, F.; Molès, J.P.; Goubaud, A.; Lemaitre, J.M.; et al. Zika Virus Strains Potentially Display Different Infectious Profiles in Human Neural Cells. *EBio Med.* **2016**, *12*, 161–169. [[CrossRef](#)]
73. Bowen, J.R.; Quicke, K.M.; Maddur, M.S.; O'Neal, J.T.; McDonald, C.E.; Fedorova, N.B.; Puri, V.; Shabman, R.S.; Pulendran, B.; Suthar, M.S. Zika Virus Antagonizes Type I Interferon Responses during Infection of Human Dendritic Cells. *PLoS Pathog.* **2017**, *13*, e1006164. [[CrossRef](#)] [[PubMed](#)]
74. Hanners, N.W.; Eitson, J.L.; Usui, N.; Richardson, R.B.; Wexler, E.M.; Konopka, G.; Schoggins, J.W. Western Zika Virus in Human Fetal Neural Progenitors Persists Long Term with Partial Cytopathic and Limited Immunogenic Effects. *Cell Rep.* **2016**, *15*, 2315–2322. [[CrossRef](#)] [[PubMed](#)]
75. Simonin, Y.; van Riel, D.; Van de Perre, P.; Rockx, B.; Salinas, S. Differential virulence between Asian and African lineages of Zika virus. *PLoS Negl. Trop. Dis.* **2017**, *11*, e0005821. [[CrossRef](#)] [[PubMed](#)]
76. Dick, G.W. Zika virus. II. Pathogenicity and physical properties. *Trans. R. Soc. Trop. Med. Hyg.* **1952**, *46*, 521–534. [[CrossRef](#)]
77. Barreto-Vieira, D.F.; Jácome, F.C.; da Silva, M.A.N.; Caldas, G.C.; de Filippis, A.M.B.; de Sequeira, P.C.; de Souza, E.M.; Andrade, A.A.; Manso, P.P.D.A.; Trindade, G.F.; et al. Structural investigation of C6/36 and Vero cell cultures infected with a Brazilian Zika virus. *PLoS ONE* **2017**, *12*, e0184397. [[CrossRef](#)]
78. Chan, J.F.W.; Yip, C.C.Y.; Tsang, J.O.L.; Tee, K.M.; Cai, J.P.; Chik, K.K.H.; Zhu, Z.; Chan, C.C.S.; Choi, G.K.Y.; Sridhar, S.; et al. Differential cell line susceptibility to the emerging Zika virus: Implications for disease pathogenesis, non-vector-borne human transmission and animal reservoirs. *Emerg. Microbes Infect.* **2016**, *5*, e93. [[CrossRef](#)]
79. Nikolay, A.; Castilho, L.R.; Reichl, U.; Genzel, Y. Propagation of Brazilian Zika virus strains in static and suspension cultures using Vero and BHK cells. *Vaccine* **2017**, in press. [[CrossRef](#)]
80. Haddow, A.D.; Schuh, A.J.; Yasuda, C.Y.; Kasper, M.R.; Heang, V.; Huy, R.; Guzman, H.; Tesh, R.B.; Weaver, S.C. Genetic characterization of Zika virus strains: Geographic expansion of the Asian lineage. *PLoS Negl. Trop. Dis.* **2012**, *6*, e1477. [[CrossRef](#)]
81. Hanada, K.; Suzuki, Y.; Gojobori, T. A large variation in the rates of synonymous substitution for RNA viruses and its relationship to a diversity of viral infection and transmission modes. *Mol. Biol. Evol. SBE* **2004**, *21*, 1074–1080. [[CrossRef](#)]
82. Holmes, E.C. Patterns of intra- and interhost nonsynonymous variation reveal strong purifying selection in dengue virus. *J. Virol.* **2003**, *77*, 11296–11298. [[CrossRef](#)]
83. Mondotte, J.A.; Lozach, P.Y.; Amara, A.; Gamarnik, A.V. Essential role of dengue virus envelope protein N glycosylation at asparagine-67 during viral propagation. *J. Virol.* **2007**, *81*, 7136–7148. [[CrossRef](#)] [[PubMed](#)]
84. Shen, S.; Shi, J.; Wang, J.; Tang, S.; Wang, H.; Hu, Z.; Deng, F. Phylogenetic analysis revealed the central roles of two African countries in the evolution and worldwide spread of Zika virus. *Virol. Sin.* **2016**, *31*, 118. [[CrossRef](#)] [[PubMed](#)]
85. Zhu, Z.; Chan, J.F.W.; Tee, K.M.; Choi, G.K.Y.; Lau, S.K.P.; Woo, P.C.Y.; Tse, H.; Yuen, K.Y. Comparative genomic analysis of pre-epidemic and epidemic Zika virus strains for virological factors potentially associated with the rapidly expanding epidemic. *Emerg. Microbes Infect.* **2016**, *5*, e22. [[CrossRef](#)] [[PubMed](#)]
86. Annamalai, A.S.; Pattnaik, A.; Sahoo, B.R.; Muthukrishnan, E.; Natarajan, S.K.; Steffen, D.; Vu, H.L.X.; Delhon, G.; Osorio, F.A.; Petro, T.M.; et al. Zika Virus Encoding Non-Glycosylated Envelope Protein is attenuated and Defective in Neuroinvasion. *J. Virol.* **2017**, *91*. [[CrossRef](#)]
87. May, M.; Relich, R.F. A Comprehensive Systems Biology Approach to Studying Zika Virus. *PLoS ONE* **2016**, *11*, e0161355. [[CrossRef](#)]
88. Wang, L.; Valderramos, S.G.; Wu, A.; Ouyang, S.; Li, C.; Brasil, P.; Bonaldo, M.; Coates, T.; Nielsen-Saines, K.; Jiang, T.; et al. From Mosquitos to Humans: Genetic Evolution of Zika Virus. *Cell Host Microbe* **2016**, *19*, 561–565. [[CrossRef](#)]
89. Pettersson, J.H.; Eldholm, V.; Seligman, S.J.; Lundkvist, A.; Falconar, A.K.; Gaunt, M.W.; Musso, D.; Nougairede, A.; Charrel, R.; Gould, E.A.; et al. How Did Zika Virus Emerge in the Pacific Islands and Latin America? *mBio* **2016**, *7*, e01239-16.24. [[CrossRef](#)]

90. Liu, Y.; Liu, J.; Du, S.; Shan, C.; Nie, K.; Zhang, R.; Li, X.F.; Wang, T.; Qin, C.F.; Wang, P.; et al. Evolutionary enhancement of Zika virus infectivity in *Aedes aegypti* mosquitoes. *Nature* **2017**, *545*, 482–486. [[CrossRef](#)]
91. Ba, F.; Loucoubar, C.; Faye, O.; Fall, G.; Mbaye, R.N.; Sembène, M.; Diallo, M.L.; Balde, A.T.; Sall, A.A.; Faye, O. Retrospective analysis of febrile patients reveals unnoticed epidemic of zika fever in Dielmo, Senegal, 2000. *Open Access Text* **2018**. [[CrossRef](#)]

Publisher’s Note: MDPI stays neutral with regard to jurisdictional claims in published maps and institutional affiliations.



© 2020 by the authors. Licensee MDPI, Basel, Switzerland. This article is an open access article distributed under the terms and conditions of the Creative Commons Attribution (CC BY) license (<http://creativecommons.org/licenses/by/4.0/>).